



Optimization of the column studies into the adsorption of basic dye using tartaric acid-treated bagasse

Ling Wei Low, Tjoon Tow Teng*, Norhashimah Morad, Baharin Azahari

School of Industrial Technology, Universiti Sains Malaysia, 11800 Minden, Penang, Malaysia

Tel. +604 6532215; Fax: +604 6573678; email: tteng@usm.my

Received 3 May 2012; Accepted 31 May 2013

ABSTRACT

Previous batch studies have shown that acid treated bagasse is a potentially useful adsorbent for treating dye wastewaters. The present paper examines the use of tartaric acid-modified bagasse for the continuous adsorption of methylene blue (MB) dye in columns. The adsorbent was characterized using Fourier transform infrared spectroscopy and scanning electron microscopy. A 2³ full factorial design analysis was carried out to screen the significant parameters that affecting the adsorption of MB dye onto tartaric acid-modified bagasse, namely initial MB concentration (100–300 mg/L), column bed height (40–80 mm), and feed flow rate (5–15 mL/min). The adsorption process was optimized using response surface methodology -central composite design with the help of Minitab[®] 14 software. Maximum decolorization (99.42%) and chemical oxygen demand reduction (88.40%) could be achieved at 200 mg/L inlet MB dye concentration with 78 mm bed height and 3.5 mL/min of feed flow rate. Thomas and Yoon–Nelson models were in good agreement with the experimental results ($r^2 > 0.91$).

Keywords: Bagasse; Methylene blue; Continuous adsorption; Optimization; Modeling

1. Introduction

The used of synthetic dyes in process industries has resulted in generation of effluents that contain highly toxic and carcinogenic compounds, high chemical oxygen demand (COD), and total organic carbon (TOC) [1]. Discharge of such effluents in water bodies not only affects esthetic nature but hinders light penetration, retards photosynthesis activity, and hence leads to the destruction of aquatic ecosystem [2,3]. Numerous physical and chemical methods have been utilized for the treatment of dyes, comprising coagulation–flocculation, liquid–liquid extraction, ozonation,

oxidation, photocatalysis, and ultrasound irradiation. Compared with the adsorption process, all these methods have some economic and environmental drawbacks, for instance, high capital and operating cost, sludge production, and complexity of the treatment processes [4,5].

Adsorption process is effective in decolorizing different types of coloring materials, removing suspended solids, odors, organic matter, and oil from aqueous solutions [6]. In recent years, a number of inexpensive alternative adsorbents from available materials, biosorbent, and waste materials from industry and agriculture, such as peanut husk [7], lotus stalks [8], mansonia wood sawdust [9,10], pecan shell [11],

*Corresponding author.

Algerian date pits [12], olive-waste cakes [13] have been investigated for possible removal of dyes from aqueous solutions as a replacement for expensive and nonrenewable commercial activated carbon [6].

In the present study, continuous adsorption in a fixed-bed column is used to measure the adsorption capacity of adsorbent. The continuous fixed-bed adsorption is different from batch adsorption experiment; fixed-bed column is simple to operate, can be scaled-up from a laboratory process, and is often desirable from an industrial point of view [14,15]. The adsorbent was prepared using an agro-lignocellulosic material (bagasse) and was modified with tartaric acid (TA) for the removal of MB dye from aqueous solution. MB is widely used in textile industries for printing calico, cotton, and dyeing leather. It can cause permanent injury to human eyes, skin, and gastrointestinal tract irritation [16].

With our knowledge from the literature survey, the used of TA modified bagasse as an adsorbent for the removal of MB dye aqueous solutions under continuous flow conditions has not been reported. Further, most previous studies used univariate (one factor at a time) method to study the factors affecting the adsorption process, which might not reach the actual optimum operational conditions. The aim of the present study is to determine the removal efficiency of TA modified adsorbent on the removal of MB dye from aqueous solution using continuous fixed-bed column. The effect of the variables i.e. column bed height, inlet MB dye concentration, and flow rate, which are affecting the adsorption process, were evaluated by using response surface methodology (RSM). The breakthrough curves for the adsorption of MB were analyzed using Adam's Bohart, Thomas, and Yoon–Nelson models.

2. Materials and methods

2.1. Preparation of tartaric acid-modified adsorbents

Bagasse was collected from a local sugarcane juice seller in Penang, Malaysia. Bagasse was washed a few times with distilled water to remove impurities and was dried under sunlight. Dried bagasse was ground to fine powder using the Retsch Mill Grinder (Rotor Beater Mill SR 200, Germany) and was sieved to obtain the particle size of 125–150 μm using Retsch Vibrator Steve Shaker (AS 200 basic, Germany). The bagasse powder was then washed with boiling distilled water until the yellowish residual water became clear.

The bagasse was then modified using TA (Bendosen, 99%) by mixing one gram of the dried bagasse

with 12 mL of 0.5 M TA. The mixture was then dried at 50°C for 24 h in an oven (Binder FD23, Germany) followed by raising the oven temperature to 120°C for 90 min for thermochemical reaction between acid and bagasse. The heated material was washed thoroughly using boiling distilled water before it was soaked in 0.1 M NaOH (R&M, 99%) in a suitable ratio and stirred for 60 min. The residual alkali was removed by performed thorough washing of bagasse with boiling distilled water until the residual solution reached the level of pH 7 and was dried at 50°C until a constant weight was achieved. The dry adsorbent was sieved to obtain the particle size of 125–150 μm and preserved in a desiccator for use [17,18].

2.2. Adsorbate

The basic dye, methylene blue (MB) ($\geq 95\%$) (Fig. 1) (C.I. 52015, chemical formula = $\text{C}_{16}\text{H}_{18}\text{ClN}_3\text{S}\cdot 2\text{H}_2\text{O}$, FW = 319.00 g/mol, $\lambda_{\text{max}} = 665 \text{ nm}$), was obtained from R&M chemicals.

2.3. Adsorbent and adsorbate characterization

2.3.1. The Fourier transform infrared (FT-IR) study

The FT-IR spectra of MB dye, raw bagasse, TA modified bagasse, and TA modified bagasse after adsorption were determined using the Potassium Bromide (KBr) disk technique, and were recorded on a Perkin-Elmer Spectrum 2000 spectrophotometer over the wavelength region 4,000–400 cm^{-1} .

2.3.2. The scanning electron microscopy (SEM) study

The morphological analysis was conducted under a voltage of 20 kV with magnification range of 50–2000 by using a Model Leo Supra 50 VP Field Emission scanning electron microscope.

2.4. Experimental set-up

A column with 2 cm inner diameter \times 50 cm length was used as vertical fixed-bed column in room temperature ($28 \pm 1^\circ\text{C}$) (Fig. 2). Samples could be taken at the height of 40–80 mm. The bottom of the column

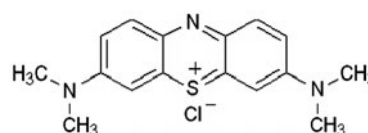


Fig. 1. Structure formula of MB dye.

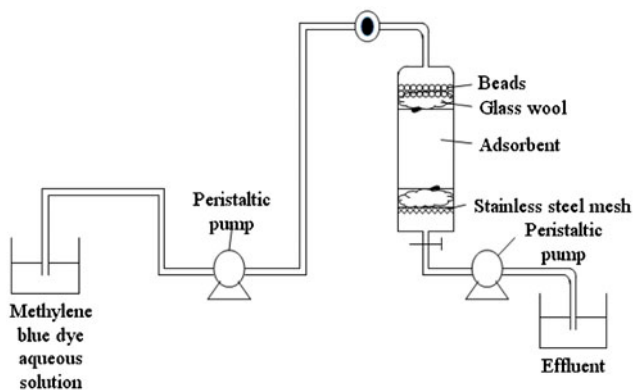


Fig. 2. Experimental set-up for fixed bed column study.

was attached with a 0.5 mm stainless steel mesh, followed by 2.0 cm glass wool. The column was then filled up with glass beads in order to provide a uniform flow of the solution through the column. MB with various concentrations (100–300 mg/L) at pH 9.0 was pumped downward through the column at a desired flow rate (5–15 mL/min) controlled by a peristaltic pump (Stenner, Model No. 85MHP5). The MB solutions at the outlet of the column were collected at a regular time intervals using the same flow rate. The outlet MB concentration was measured using a Shimadzu UV visible spectrophotometer (Model UV-1601 PC) at 665 nm and was analyzed to yield output concentration breakthrough curves. The COD was determined through closed reflux, colorimetric method based on the standard methods for the examination of water and wastewater [19]. The experiments were repeated thrice at the same experimental conditions.

The amount of MB adsorbed onto the adsorbent was calculated by the following mass balance relationship [1]:

$$q_e = \frac{(C_0 - C_e)V}{W} \quad (1)$$

The decolorization efficiency was calculated by the formula [1]:

$$\text{Color (\%)} = \frac{100(C_0 - C_e)}{C_0} \quad (2)$$

where q_e is the amount (mg/g) of MB adsorbed at equilibrium, C_0 and C_e are the initial and equilibrium liquid-phase concentration of MB (mg/L), respectively, V is the volume of solution (L), and W is the mass of the adsorbent (g).

The COD reduction efficiency was calculated using [1]:

$$\text{COD (\%)} = \frac{100(J_a - J_b)}{J_a} \quad (3)$$

where J_a is the initial COD concentration (mg/L) and J_b is the equilibrium COD concentration (mg/L).

2.5. Modeling of column data

2.5.1. Thomas model

The Thomas model [20] assumes plug flow behavior in the column [3,15]. This model is one of the most general methods applied in the column performance theory. It is widely applied in the processes where the external and internal diffusion limitations are absent [3]. The Thomas model can be expressed as [15]:

$$\ln\left(\frac{C_0}{C_t} - 1\right) = \frac{k_{Th}q_e w}{Q} - k_{Th}C_0 t \quad (4)$$

where k_{Th} (mL/min mg) is the Thomas rate constant; q_e (mg/g) is the equilibrium MB uptake per gram of the adsorbent; C_0 (mg/L) is the inlet MB dye concentration; C_t (mg/L) is the effluent concentration at time t ; w (g) the mass of adsorbent; Q (mL/min) the flow rate, and t (min) is the flow time. The value of C_0/C_t is the ratio of inlet and outlet MB concentrations. The values of k_{Th} and q_e can be determined from the slope and the intercept, respectively, of the linear plot of $\ln[(C_0/C_t) - 1]$ vs. time t .

2.5.2. Adams–Bohart model

The Adams–Bohart model [21] assumes that the adsorption rate is proportional to both the residual adsorbent capacity and the adsorbate concentration. This model is used for the description of the initial part of the breakthrough curve [3,15]. The Adams–Bohart model can be defined as [15]:

$$\ln\frac{C_t}{C_0} = k_{AB}C_0 t - k_{AB}N_0\frac{Z}{F} \quad (5)$$

where C_0 and C_t (mg/L) are the inlet and effluent MB dyes concentration, respectively; k_{AB} (L/mg min) is the Adam-Bohart rate constant, F (cm/min) is the linear velocity. F value is calculated by dividing the flow rate by the column section area, Z (cm) is the bed depth of column, and N_0 (mg/L) is the saturation concentration. The values of k_{AB} and N_0 can be obtained from the slope and intercept, respectively, of a linear plot of $\ln(\frac{C_t}{C_0})$ against time (t).

2.5.3. Yoon–Nelson model

The Yoon–Nelson model assumes that the rate of decrease in the probability of adsorption for each adsorbate molecule is proportional to the probability of adsorbate adsorption and the probability of adsorbate breakthrough on the adsorbent [22]. Yoon–Nelson model can be expressed as [3,23]:

$$\ln \frac{C_t}{C_0 - C_t} = k_{YN}t - \tau k_{YN} \quad (6)$$

where k_{YN} (1/min) is the rate velocity constant; τ (min) is the time required for 50% adsorbate breakthrough. The values of k_{YN} and τ can be obtained from the slope and intercept, respectively, of a plot of $\frac{C_t}{(C_0 - C_t)}$ vs. sampling time (t).

2.6. Design of experiment

RSM was carried out to study the effect of three factors (independent variables): bed height (x_1), inlet MB concentration (x_2), and feed flow rate (x_3) on decolorization (y_1) and COD reduction (y_2). RSM is a combination of statistical and mathematical techniques used for the study of several control variables simultaneously [24]. RSM contain three main steps, namely design and experiments, response surface modeling through regression, and optimization [25]. The main objective of RSM is to determine the optimum operational conditions of the adsorption process or to identify a region that satisfies the operating specifications [25]. Application of RSM in the present study can result in closer confirmation of the output response, reduced process variability, and reduced development time and overall costs [26]. Central Composite Design (CCD) is often used in RSM to fit a model by least squares technique [27]. CCD can be defined as a rotatable design that provides equal precision for fitted response at points (factor level combinations) that are at equal distances from the center of the factor space [28].

Data from the CCD were subjected to a second-order multiple regression analysis to explain the behavior of the system using the least squares regression methodology for obtaining the parameter estimators of the mathematical model [25,29]:

$$y = f(x_1, x_2, x_3) + \varepsilon \quad (7)$$

The response y is a function of the levels of independent variables:

where ε represents the error observed in the response y . The expected response is:

$$E(y) = f(x_1, x_2, x_3) = \eta \quad (8)$$

and the surface area is represented by:

$$\eta = f(x_1, x_2, x_3) \quad (9)$$

where η is a response surface. Experimental data were analyzed to fit the following second-order model:

$$\eta = \beta_0 + \sum_{i=1}^k \beta_i x_i + \sum_{i=1}^k \beta_{ii} x_i^2 + \sum_{i < j} \beta_{ij} x_i x_j \quad (10)$$

where β_0 , β_i , β_{ii} , and β_{ij} are regression coefficients, and x_i are the coded variables. The relationship between the natural variable ζ_i and the coded variables x_i can be represented by:

$$x_i = \frac{\zeta_i(\text{High level} + \text{Low level})/2}{(\text{High level} - \text{Low level})/2} \quad (11)$$

3. Results and discussion

3.1. Effect of initial pH value

The initial pH value of the dye solution was adjusted to pH 9.4. This is because from our previous optimization study using RSM, the optimal pH for the removal of MB using TA modified bagasse was fall at pH 9.4 [18]. MB is a basic dye. Adsorption of these positively charged dye groups onto adsorbent surface are influenced by the surface charge on the adsorbent [1]. When the solution is in the acidic condition, the number of negative charges on the adsorbent sites increased and positive charge decreased which did not favor the adsorption of positively charged dye cations due to electrostatic repulsion [18,30].

3.2. Effect of initial dye concentration

The effect of the influent MB concentration on the shape of the breakthrough curves was studied by plotting C_t/C_0 vs. t in Fig. 3. Various influent MB dye concentrations (100–300 mg/L) were used with the same solution flow rate of 5 mL/min and adsorbent bed height of 80 mm. Fig. 3 shows that in the interval of 60 min, the value of C_t/C_0 reached 0.59, 0.82, and 0.93 when the inlet MB concentration was 100, 200, and 300 mg/L, respectively. The breakthrough time slightly decreased with influent MB dye concentration. At lower influent MB concentrations, breakthrough curves were dispersed and breakthrough occurred slowly. However, when the influent

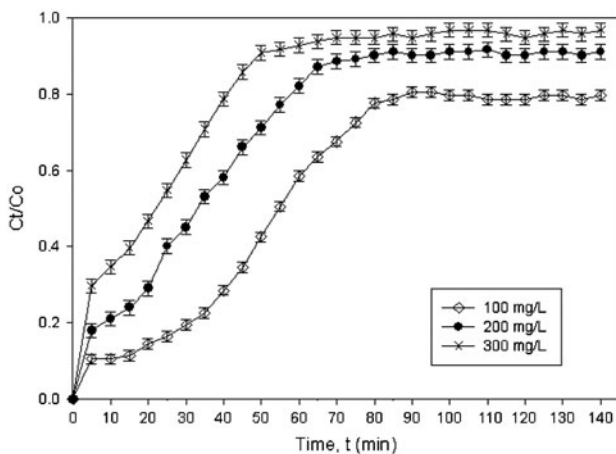


Fig. 3. Breakthrough curves for MB adsorption on TA modified bagasse at different initial dye concentrations.

MB concentration increased, sharper breakthrough curves were obtained. Similar trends were obtained for biosorption of MB by rice husk [31] removal of reactive azo dye onto granular activated carbon prepared from waste [15], removal of MB by phoenix tree leaf powder [3], and removal of acid dye using pristine and acid-activated clays [32]. This is due to more adsorption sites were being covered as MB concentration increases [3]. A lower concentration gradient led to a slower transport due to a decrease in the diffusion coefficient or mass transfer coefficient [15]. The higher the inlet MB concentration, the steeper is the breakthrough curve slope, and the smaller is the breakthrough time. These results explained that the changes of the concentration gradient will affect the saturation rate and breakthrough time. This also shows that the diffusion process is concentration dependent [15]. As the influent MB concentration increases, MB loading rate also increases; this will increase the driving force for mass transfer which decreases the adsorption zone length [33].

3.3. Effect of column bed height

Fig. 4 shows the breakthrough curves obtained for MB adsorption on TA modified bagasse by using different column bed height of 40, 60, and 80 mm (4.68, 6.07, and 7.53 g), at a constant flow rate of 5 mL/min and inlet MB concentration of 100 mg/L. The breakthrough and time increased with the bed height (Fig. 4). When the bed height increases, MB had more time to contact with TA modified bagasse, which resulted in higher removal efficiency of MB dye in column [34]. Therefore, higher bed column

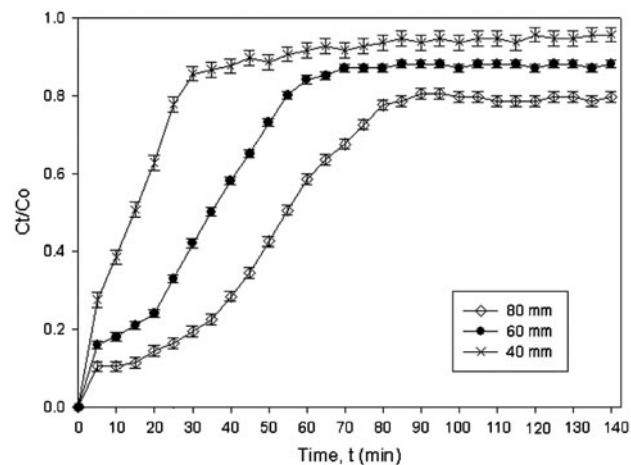


Fig. 4. Breakthrough curves for MB adsorption on TA modified bagasse for different bed heights.

results in a lower effluent concentration at the same time. The slope of the breakthrough curve decreased with increasing bed height, which resulted in broaden mass transfer zone [3,15]. High adsorption capacity was observed at the highest bed height. This is because, increase in the surface area provided more binding sites for adsorption [34,35].

3.4. Effect of feed flow rate

The effect of feed flow rate on the adsorption of MB using the TA modified bagasse was investigated by varying the flow rate (5, 10, and 15 mL/min) with a constant adsorbent bed height of 8 cm and the inlet MB concentration of 100 mg/L, as shown by the breakthrough curve in Fig. 5. It can be seen that the breakthrough generally occurred faster with a higher flow rate. The breakthrough time reaching saturation was decreased significantly with increased in the flow rate [36]. At lower flow rate, MB dye will have more time to contact with TA modified bagasse and hence resulted in higher removal of MB dye in column. Mass transfer fundamentals can be used to explain the variation in the slope of the breakthrough curve and adsorption capacity. When the flow rate is high, the mass transfer rate will increase, i.e. the amount of dye adsorbed onto unit bed height (mass transfer zone) get increased with flow rate, leading to faster saturation of the column at higher flow rate [15,36]. Higher flow rate lead to lower adsorption capacity due to insufficient residence time of the MB dye in the column and diffusion of the solute left the column before equilibrium occurred [37].

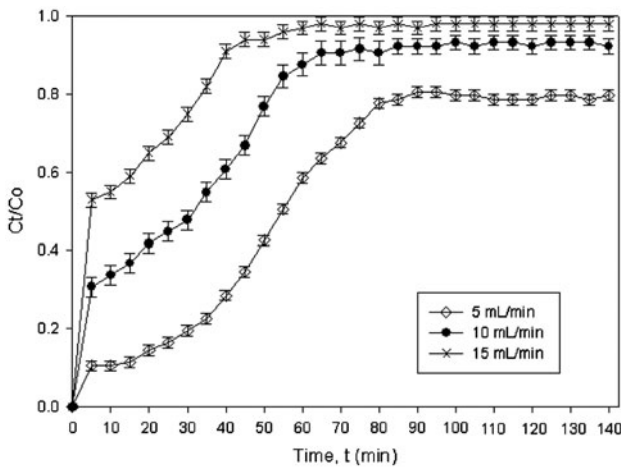


Fig. 5. Breakthrough curves for MB adsorption on TA modified bagasse at different flow rates.

3.5. Dynamic adsorption models

3.5.1. Thomas model

The column data were fitted to the Thomas model to determine the Thomas rate constant (k_{Th}) and maximum solid-phase concentration (q_e). The determined coefficients and relative constants were obtained using linear regression analysis according to Eq. (4). A linear plot of $\ln[(C_0/C_t) - 1]$ against time (t) was used to determine the values of k_{Th} and q_e from the slope and intercept, respectively, of the plot. The results are listed in Table 1. As shown in Table 1, the results were all fits with high determination coefficients (r^2) ranging from 0.89 to 0.98. When the inlet MB dye concentration increased from 100 to 300 mg/L, the value of q_e decreased but the value of k_{Th} increased. This is because the driving force for adsorption is the concentration difference between the dye on the adsorbent and the dye in the solution [15,23,38]. As the bed depth increases, the value of q_e increased, but

the value of k_{Th} decreased. With increasing flow rate, the value of q_e decreased, but the value of k_{Th} increased. The results show that with lower flow rate, lower initial dye concentration and higher bed heights would increase the adsorption of MB on the TA modified adsorbent column. The data can be well described by Thomas model, where the external and internal diffusions will not be the limiting step [23].

3.5.2. The Adam's Bohart model

The Adam's Bohart Model was applied to experimental data to describe the initial part of the breakthrough curve. The values of N_0 and k_{AB} were calculated from the plot of $\ln(\frac{C_t}{C_0})$ against time (t) (Eq. (5)) and the values are presented in Table 2 together with the determination coefficients. From Table 2, the value of k_{AB} increased with both initial MB concentration and flow rate, but it decreased with increasing bed height. The value of N_0 decreased with initial MB concentration and bed height, but increased with flow rate. These showed that the overall system kinetics was dominated by external mass transfer in the initial part of adsorption in the column [3,23].

3.5.3. The Yoon–Nelson model

A simple theoretical model developed by Yoon–Nelson was applied to determine the breakthrough behavior of MB on TA modified adsorbent. The values of a rate constant (k_{YN}) and the time required for 50% MB breakthrough (τ) could be obtained from the slope and intercept of a linear plot of $\ln[C_t/(C_0 - C_t)]$ against sampling time (t) (Eq. (6)). The values of k_{YN} and τ are listed in Table 3. From the table, the values of the rate constant k_{YN} increased and the 50% breakthrough time τ decreased with both increasing MB inlet concentration and flow rate. When the bed height increased, the value of τ increased while k_{YN} decreased.

Table 1
Calculated constants of the Thomas model at different conditions using linear regression analysis

Inlet MB dye concentrations (mg/L)	Bed height (mm)	Flow rate (mL/min)	Value of k_{Th} (mL/min mg) $\times 10^3$	Value of q_e (mg/g) $\times 10^{-2}$	r^2
100	80	5	4.45	12.94	0.98
200	80	5	8.98	3.80	0.95
300	80	5	13.98	1.22	0.92
100	60	5	4.48	10.90	0.92
100	40	5	4.86	2.35	0.89
100	80	10	4.54	10.17	0.91
100	80	15	5.55	1.66	0.94

Table 2
Adams–Bohart parameters at different conditions using linear regression analysis

Inlet MB dye concentrations (mg/L)	Bed height (mm)	Flow rate (mL/min)	Value of k_{AB} (L/mg.min) $\times 10^3$	Value of N_0 (mg/L)	r^2
100	80	5	2.5	5.81	0.94
200	80	5	3.36	2.65	0.83
300	80	5	3.39	1.68	0.76
100	60	5	0.91	9.71	0.59
100	40	5	1.84	7.06	0.81
100	80	10	1.2	10.62	0.87
100	80	15	0.63	15.21	0.75

Table 3
Yoon–Nelson parameters at different conditions using linear regression analysis

Inlet MB dye concentrations (mg/L)	Bed height (mm)	Flow rate (mL/min)	k_{YN} (1/min)	τ (min)	r^2
100	80	5	0.0445	57.98	0.98
200	80	5	0.0449	34.01	0.95
300	80	5	0.0466	16.36	0.92
100	60	5	0.0448	36.61	0.92
100	40	5	0.0486	5.27	0.89
100	80	10	0.0454	22.78	0.91
100	80	15	0.0457	1.65	0.88

Both Thomas and Yoon–Nelson model provide the better fit ($r^2 > 0.91$) to the experimental data at various condition (Tables 1 and 3). Hence, Thomas and Yoon–Nelson models can be used to describe the behavior of the adsorption of MB in a TA modified adsorbent fixed-bed column. The value of r^2 for Adams–Bohart model is slightly lower than that of Thomas and Yoon–Nelson model under the same experimental conditions.

3.6. Optimization of the fixed-bed column study

3.6.1. Screening of process variables in fixed-bed column study

A 2^3 full factorial design was used for screening of important factors affecting the MB dye adsorption in the fixed-bed column. The factors and levels used in this experiment are presented in Table 4. The range of values for each factors were determined based on preliminary experiments. All factors (inlet MB dye concentration, adsorbent bed height, and feed flow rate) showed significant effect on decolorization and COD reduction of MB dye adsorption on TA modified bagasse. Therefore, all factors were used in the analysis for the next step.

3.6.2. Optimization of adsorption study: fixed-bed column study

The three parameters (inlet MB dye concentration, column bed height, and feed flow rate) that have significant effect on the adsorption of MB dye using TA modified bagasse on column studies in terms of percentage of color removal and COD reduction were further investigated in optimizing the adsorption process.

A two-level CCD with 36 runs was used. The results of the 60 runs with three variables and three replications are given in Table 5.

Table 4
Experimental ranges and levels for full factorial design (fixed-bed column study)

Factors	Levels	
	Low level (–)	High level (+)
A: Inlet MB dye concentration	100 mg/L	300 mg/L
B: Bed height	40 mm	80 mm
C: Feed flow rate	5 mL/min	15 mL/min

Table 5
CCD in natural variables with the experimental data values of percentage color removal and COD reduction (fixed-bed column study)

Input variables			Response	
x_1 Inlet MB concentration (mg/L)	x_2 Bed height (mm)	x_3 Flow rate (mL/min)	y_1 (%)	y_2 (%)
200	94	10	85.19	80.80
200	26	10	40.63	36.24
368	60	10	67.71	63.32
100	80	15	54.55	49.55
368	60	10	67.23	62.98
200	26	10	40.97	36.71
200	60	18.5	48.14	43.89
200	60	18.5	49.72	45.87
200	60	10	65.48	61.24
200	60	10	66.86	60.28
100	40	15	16.98	11.03
200	26	10	39.41	34.87
200	60	10	74.69	70.25
200	60	10	68.78	60.22
68	60	10	32.18	27.70
100	40	5	32.00	25.67
300	80	5	93.45	86.09
200	60	10	81.19	76.00
200	60	10	76.29	72.13
200	60	10	66.49	61.20
200	94	10	86.73	85.28
300	40	5	56.79	50.43
300	40	15	45.98	39.62
68	60	10	33.29	29.00
200	60	18.5	44.79	41.29
100	40	15	17.39	12.04
100	40	15	20.23	13.87
100	80	5	71.23	64.87
368	60	10	58.74	55.78
200	60	10	80.01	75.32
200	60	10	63.07	59.84
200	60	10	67.07	64.28
100	80	15	60.53	55.00
300	80	5	93.00	87.21
300	80	15	65.68	60.34
200	60	10	81.00	76.46
300	40	15	47.81	41.46
300	80	15	64.48	58.42
68	60	10	30.03	26.89
100	40	5	35.67	29.29
100	80	15	56.91	51.32
200	60	10	79.29	72.31
300	40	15	44.37	39.00

(Continued)

Table 5
(Continued)

Input variables			Response	
x_1 Inlet MB concentration (mg/L)	x_2 Bed height (mm)	x_3 Flow rate (mL/min)	y_1 (%)	y_2 (%)
100	80	5	73.38	67.04
300	40	5	58.92	51.51
200	60	10	82.95	77.71
200	60	10	75.39	71.68
100	80	5	75.00	69.45
200	60	3.5	83.46	78.46
200	60	3.5	84.37	80.00
300	80	5	91.24	85.32
300	80	15	66.54	61.19
200	94	10	88.39	84.32
200	60	10	78.04	72.13
200	60	10	85.64	84.29
200	60	3.5	81.07	76.26
100	40	5	34.79	29.31
300	40	5	60.03	53.68
200	60	10	83.13	83.28

The second-order models for the percentage of color removal (y_1) and the percentage of COD reduction (y_2) in terms of coded variables are shown in Eqs. (12) and (13), respectively.

$$y_1 = 74.7236 + 9.8790x_1 + 15.3599x_2 - 9.5859x_3 - 9.8473x_1^2 - 4.4179x_2^2 - 3.8151x_3^2 - 3.0854x_1x_2 - 0.9621x_1x_3 - 1.7988x_2x_3 \quad (12)$$

$$y_2 = 69.8002 + 9.7990x_1 + 15.5888x_2 - 9.3087x_3 - 9.9005x_1^2 - 4.4470x_2^2 - 4.0021x_3^2 - 3.0479x_1x_2 - 0.8912x_1x_3 - 1.7204x_2x_3 \quad (13)$$

where y is the predicted response, x_1, x_2, x_3 —coded values of the factors, (x_1 =inlet MB concentration, x_2 = column bed height, x_3 = feed flow rate).

The second-order regression model obtained for color removal and COD reduction is satisfied, since the values of the coefficient of determination (r^2) are high and close to 1. The r^2 values for the percentage of color removal and COD reduction are 94.80 and 92.90%, respectively. The ANOVA shows the second-order model adequately fitted the experimental data (Table 6) with lack of fit values larger than 0.5. The

Table 6
ANOVA for percentage of color removal and COD reduction

Source	DF	Adj SS	Adj MS	F	P
% Color removal					
Linear	3	17429.30	5809.78	231.90	0.000
Quadratic	3	4990.10	1663.36	66.39	0.000
Interaction	3	328.30	109.45	4.37	0.008
Residual error	50	1252.70	25.05		
Lack-of-Fit	5	228.70	45.74	2.01	0.595
Total	59				
% COD reduction					
Linear	3	17440.40	5813.46	167.03	0.000
Quadratic	3	5084.10	1694.71	48.69	0.000
Interaction	3	313.10	104.35	3.00	0.039
Residual error	50	1740.20	34.80		
Lack-of-Fit	5	358.00	71.60	2.33	0.658
Total	59				

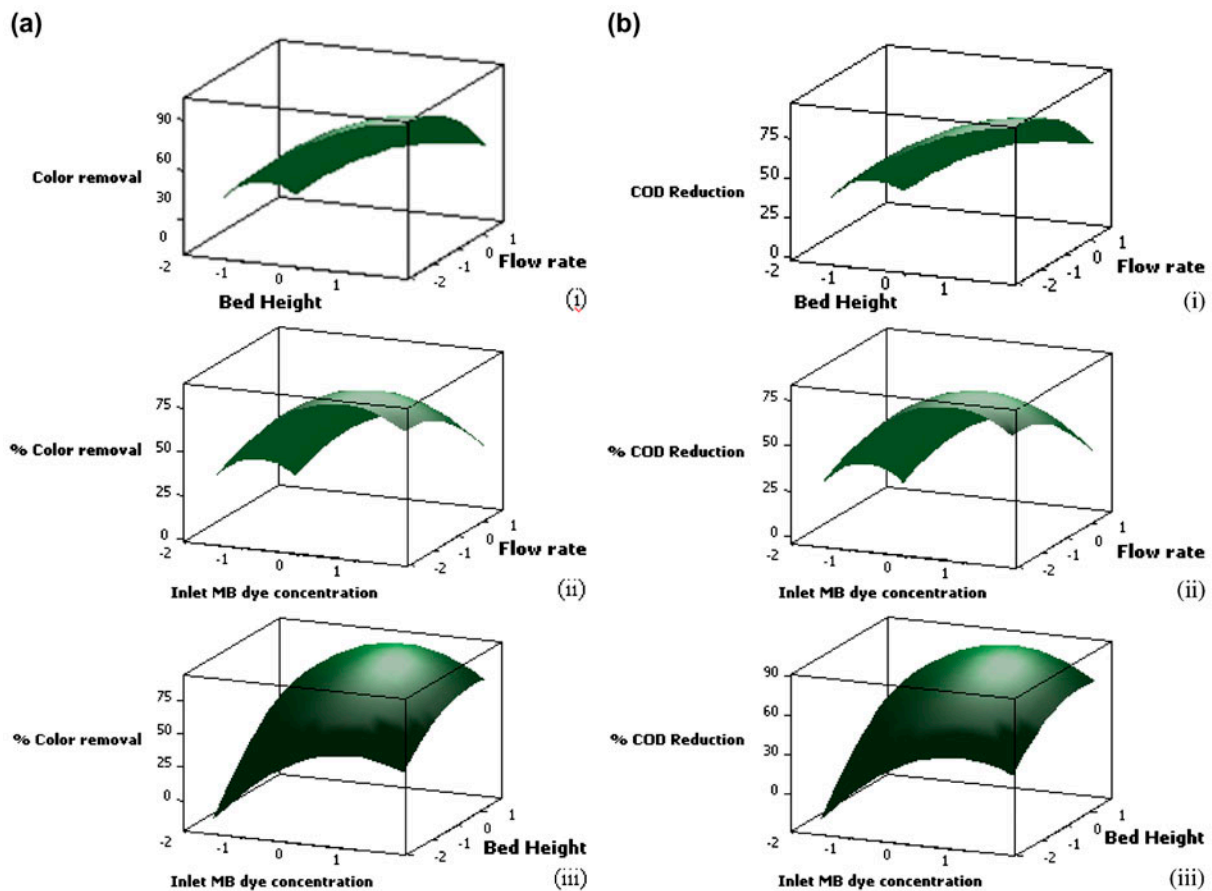


Fig. 6. Three-dimensional response surface plot for (a)% color removal (b)% COD reduction as a function of bed height and flow rate (i), inlet MB dye concentration and flow rate (ii), and inlet MB dye concentration and bed height (iii).

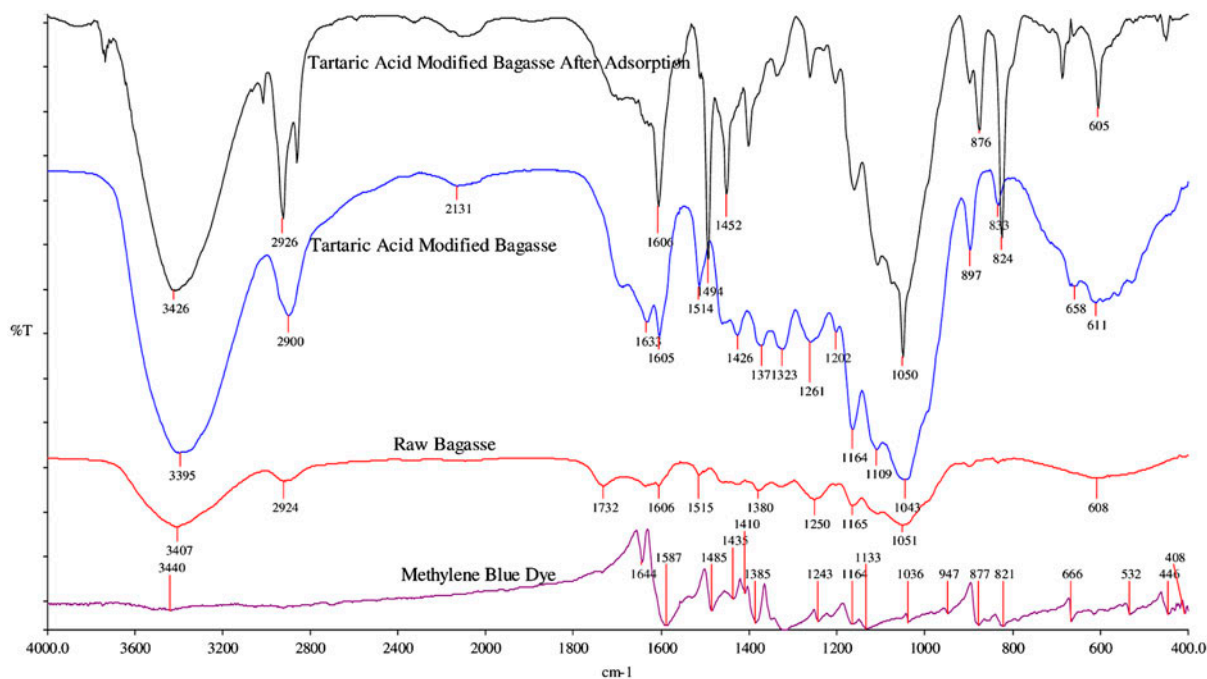


Fig. 7. Adsorption peaks for MB, raw bagasse, TA modified bagasse, and TA modified bagasse after adsorption process.

linear effect of selected factor is significant ($p < 0.0001$). The quadratic effect over the linear effect and two factor interactions between different factors are significant with $p < 0.0001$.

The three-dimensional response surface plot for decolorization and COD reduction is given in Fig. 6 as a function of bed height and flow rate (i), inlet MB dye concentration and flow rate (ii), and inlet MB dye concentration and bed height (iii) at an intermediate setting of 200 mg/L inlet MB dye concentration, 60 mm bed height, and 10 mL/min feed flow rate. The figures exhibit a clear peak, indicating the ability of maximizing the decolorization and COD reduction process within the selected levels of factors under study. The optimum condition for maximum decolorization and COD reduction is well defined inside the design boundary.

3.6.3. Optimization of the fixed-bed column experiment

Based on the above discussion, an optimization study was carried out to determine the optimal conditions for decolorization and COD reduction of MB dye aqueous solution in column study. In fact, once the model has been developed and checked for adequacy, the optimization criteria can be set to find the optimum conditions [16]. The highest percentage of color removal (94.22%) and percentage of COD

reduction (88.40%) could be achieved by setting the level of process variables at 201.7 mg/L inlet MB dye concentration, 78 mm bed height, and 3.5 mL/min of feed flow rate.

3.7. FT-IR spectroscopy analysis

During TA modification, the surface functional groups of the bagasse adsorbent significantly experienced chemical changes. Fig. 7 shows the FT-IR spectra of the raw bagasse, MB dye, TA modified bagasse before and after adsorption process. FT-IR peaks in MB dye are 3,440 cm^{-1} for the NH_2 aromatic group, 1,644 cm^{-1} for amines secondary group, 1,485 cm^{-1} for phenyl group, 1,410 cm^{-1} for the $-\text{CONH}_2$ group, 1,435 cm^{-1} for the R-OH group, 947 cm^{-1} for $-\text{C}-\text{OH}$ group, and 532 cm^{-1} for the Chloro C-Cl group. After TA modification, a few peaks, which were also found in raw bagasse, such as hydroxyl group, vinyl ethers group, aromatic compounds, phenolic group, $-\text{C}-\text{O}-\text{C}-$ group, sulfoxides group, $\text{Si}-\text{CH}_3$ group, and C-Br group have shifted. Some new functional groups, such as carboxylic group (2,900 and 1,428 cm^{-1}), aldehydes (1,733 cm^{-1}), and $-\text{SO}_2\text{Cl}$ (1,376 cm^{-1}) were formed. These spectroscopic results showed that the introduction of the new functional groups through TA modification may effectively convert bagasse to highly adsorbing materials. After the adsorption process,

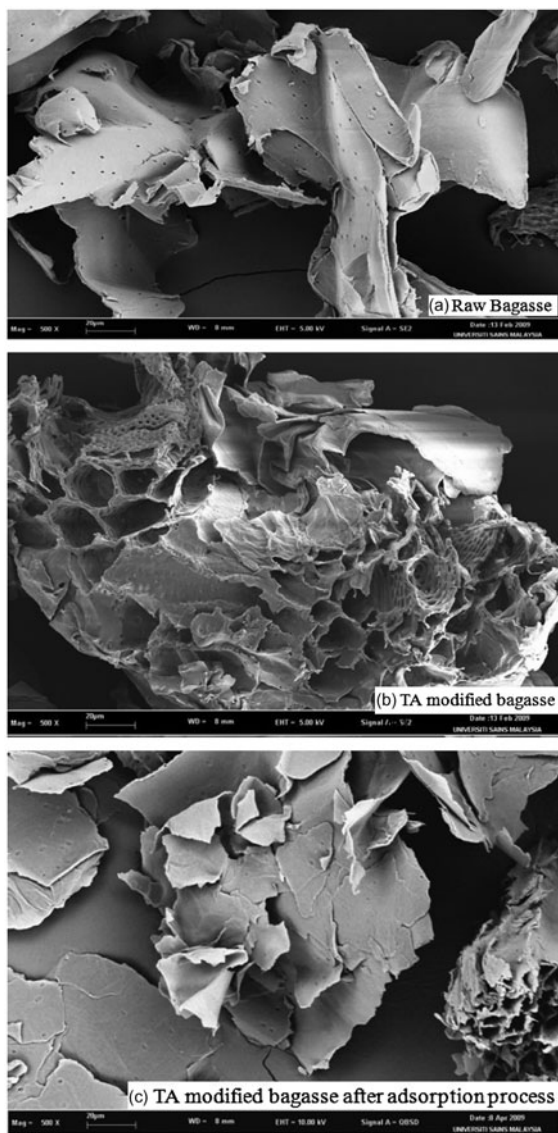


Fig. 8. Scanning electron microscope of (a) Raw Bagasse (b) TA modified bagasse (c) TA modified bagasse after adsorption process (magnification: 500 \times).

peaks that were found in MB were also noticed in TA modified bagasse, namely 3,426, 1,494, 1,402, and 1,452 cm^{-1} . This shows that MB dye has been adsorbed onto the TA modified bagasse.

3.8. SEM analysis

The surface structure of bagasse was analyzed by SEM before and after acid modification and after adsorption process with a magnification of 500 \times . Fig. 8(a) shows that before TA modification the surface of the bagasse was smooth with a few tiny pores.

However, after TA modification (Fig. 8(b)) surface morphological modification can be seen. The surface became uneven with a few pores. Fig. 8(c) shows SEM micrographs of TA modified bagasse after adsorption process. The surfaces became rough as they were covered by dye molecules.

4. Conclusion

The present study identified TA modified bagasse as a suitable adsorbent to be used for continuous removal of MB from aqueous solutions. The optimum column adsorption conditions (94.22% of color removal, and 88.40% of COD reduction) could be achieved by setting the level of process variables at 201.7 mg/L inlet MB dye concentration, 78 mm bed height, and 3.5 mL/min of feed flow rate. The fixed-bed adsorption system was found to perform well with lower initial MB dye concentration, higher adsorbent bed height, and lower feed flow rate. As the influent MB concentration increases, MB loading rate also increases, this will increase the driving force for mass transfer which decreases the adsorption zone length. High adsorption capacity was observed at the highest bed height. This is because, increase in the surface area provided more binding sites for adsorption. Higher flow rate lead to lower adsorption capacity due to insufficient residence time of the MB dye in the column and diffusion of the solute left the column before equilibrium occurred. The adsorption of MB dye using TA modified bagasse in fixed-bed column can be well described by Thomas ($r^2 > 0.89$) and Yoon–Nelson ($r^2 > 0.88$) models, where the external and internal diffusions will not be the limiting step.

Acknowledgement

The authors acknowledge the research grant provided by Malayan Sugar Manufacturing Company under Kuok Foundation Berhad and the research facilities of Universiti Sains Malaysia (USM).

References

- [1] X.S. Wang, Y. Zhou, Y. Jiang, C. Sun, The removal of basic dye from aqueous solutions using agricultural by-products, *J. Hazard. Mater.* 157 (2008) 374–385.
- [2] K. Kadirvelu, M. Palanival, R. Kalpana, S. Rajeswar, Activated carbon from an agricultural by-product for the treatment of dyeing industry wastewater, *Bioresour. Technol.* 74 (2000) 263–265.
- [3] R.P. Han, Y. Wang, X. Zhao, Y.F. Wang, F.L. Xie, J.M. Cheng, M.S. Tang, Adsorption of methylene blue by phoenix tree leaf powder in a fixed-bed column: Experiments and prediction of breakthrough curves, *Desalination* 245 (2009) 284–297.

- [4] A. Talebi, T.T. Teng, A.F.M. Alkarkhi, I. Norli, L.W. Low, Optimization of nickel removal using liquid-liquid extraction and response surface methodology, *Desalin. Water Treat.* 47 (2012) 334–340.
- [5] M. Toor, B. Jin, Adsorption characteristics, isotherm, kinetics, and diffusion of modified natural bentonite for removing diazo dye, *Chem. Eng. J.* 187 (2012) 79–88.
- [6] G. Crini, Non-conventional low-cost adsorbents for dye removal: A review, *Bioresour. Technol.* 97 (2006) 1061–1085.
- [7] W. Zou, H. Bai, S. Gao, X. Zhao, R. Han, Investigations on the batch performance of cationic dyes adsorption by citric acid modified peanut husk, *Desalin. Water Treat.* 49 (2012) 41–56.
- [8] L.H. Huang, Y.Y. Sun, Q.K. Yue, Q.Y. Yue, L. Li, B. Gao, Adsorption of Cd (II) on lotus stalks-derived activated carbon: Batch and column studies, *Desalin. Water Treat.* 41 (2012) 122–130.
- [9] A.E. Ofomaja, Kinetic study and sorption mechanism of methylene blue and methyl violet onto mansonia (*Mansonia altissima*) wood sawdust, *Chem. Eng. J.* 143 (2008) 85–95.
- [10] A.E. Ofomaja, Kinetic and pseudo-isotherm studies of 4-nitrophenol adsorption onto mansonia wood sawdust, *Ind. Crops Prod.* 33 (2011) 418–428.
- [11] K.T. Klasson, L.H. Wartelle, J.E. Rodgers, III, I.M. Lima, Copper (II) adsorption by activated carbons from pecan shells: Effect of oxygen level during activation, *Ind. Crops Prod.* 30 (2009) 72–77.
- [12] N. Bouchemal, Y. Azoudj, Z. Merzougui, F. Addoun, Adsorption modeling of Orange G dye on mesoporous activated carbon prepared from Algerian date pits using experimental designs, *Desalin. Water Treat.* 45 (2012) 284–290.
- [13] R. Baccar, P. Blanquez, J. Bouzid, M. Feki, H. Attiya, M. Sara, Modeling of adsorption isotherms and kinetics of a tannery dye onto an activated carbon prepared from an agricultural by-product, *Fuel Process. Technol.* 106 (2013) 408–415.
- [14] J.M. Chern, Y.W. Chien, Adsorption of nitrophenol onto activated carbon: Isotherms and breakthrough curves, *Water Res.* 36 (2002) 647–655.
- [15] A.A. Ahmad, B.H. Hameed, Fixed-bed adsorption of reactive azo dye onto granular activated carbon prepared from waste, *J. Hazard. Mater.* 175 (2010) 298–303.
- [16] O. Hamdaoui, M. Chiha, Removal of methylene blue from aqueous solutions by wheat bran, *Acta Chim. Slov.* 54 (2007) 407–418.
- [17] L.W. Low, T.T. Teng, A. Anees, M. Norhashimah, Optimization of the adsorption conditions for the decolorization and COD reduction of methylene blue aqueous solution using low-cost adsorbent, *Water Air Soil Pollut.* 214 (2011) 185–195.
- [18] L.W. Low, T.T. Teng, A. Anees, M. Norhashimah, Y.S. Wong, A novel pretreatment method of lignocellulosic material as adsorbent and kinetic study of dye waste adsorption, *Water Air Soil Pollut.* 218 (2011) 293–306.
- [19] APHA, Standard Methods for the Examination of Water and Wastewater, 21st ed., American Public Health Association (APHA), American Water Works Association (AWWA) and Water Environment Federation (WEF), Washington, DC, 2005.
- [20] H.C. Thomas, Heterogeneous ion exchange in a flowing system, *J. Am. Chem. Soc.* 66 (1944) 1466–1664.
- [21] G.S. Bohart, E.Q. Adams, Behavior of charcoal towards chlorine, *J. Chem. Soc.* 42 (1920) 523–529.
- [22] Y.H. Yoon, J.H. Nelson, Application of gas adsorption kinetics. Part I. A theoretical model for respirator cartridge service time, *Am. Ind. Hyg. Assoc. J.* 45 (1984) 509–516.
- [23] Z. Aksu, F. Gonen, Biosorption of phenol by immobilized activated sludge in a continuous packed bed: Prediction of breakthrough curves, *Process Biochem.* 39 (2004) 599–613.
- [24] M.A. Bezerra, R.E. Santelli, E.P. Oliveira, L.S. Villar, L.A. Escalera, Response surface methodology (RSM) as a tool for optimization in analytical chemistry, *Talanta* 76 (2008) 965–977.
- [25] S.H. Hasan, P. Srivastava, M. Talat, Biosorption of lead using immobilized *Aeromonas hydrophila* biomass in up flow column system: Factorial design for process optimization, *J. Hazard. Mater.* 177 (2010) 312–322.
- [26] M.Y. Can, Y. Kaya, O.F. Algur, Response surface optimization of the removal of nickel from aqueous solution by cone biomass of *Pinus sylvestris*, *Bioresour. Technol.* 97 (2006) 1761–1765.
- [27] D.C. Montgomery, Design and analysis of experiments, 5th ed., John Wiley & Sons, New York, 2001.
- [28] V.V. Karunakaran, Quality assurance and optimization studies of light weight PU prosthetic foot, *Trends Biomater. Artif. Organs* 19 (2006) 63–69.
- [29] A. Kumar, B. Prasad, I.M. Mishra, Optimization of process parameter for acrylonitrile removal by low cost adsorbent using Box-Behnken design, *J. Hazard. Mater.* 150 (2008) 174–182.
- [30] C. Nainasivayam, K. Kadirvelu, Coir pith, an agricultural waste by-product for the treatment of dyeing wastewater, *Bioresour. Technol.* 48 (1994) 79–81.
- [31] R. Han, Y. Wang, W. Yu, W. Zou, J. Shi, H. Liu, Biosorption of methylene blue from aqueous solution by rice husk in a fixed-bed column, *J. Hazard. Mater.* 141 (2007) 713–718.
- [32] S.H. Lina, R.S. Juang, Y.H. Wang, Adsorption of acid dye from water on pristine and acid activated clays in fixed beds, *J. Hazard. Mater.* 113 (2004) 195–200.
- [33] J. Goel, K. Kadirvelu, C. Rajagopal, V.K. Garg, Removal of lead (II) by adsorption using treated granular activated carbon: Batch and column studies, *J. Hazard. Mater.* 125 (2005) 211–220.
- [34] Z. Zulfadhly, M.D. Mashitah, S. Bhatia, Heavy metals removal in fixed-bed column by the macro fungus *Pycnoporus sanguineus*, *Environ. Pollut.* 112 (2001) 463–470.
- [35] K. Vijayaraghavan, J. Jegan, K. Palanivelu, M. Velan, Removal of nickel(II) ions from aqueous solution using crab shell particles in a packed bed up flow column, *J. Hazard. Mater.* 113B (2004) 223–230.
- [36] C.K. Ko, J.F. Porter, G. McKay, Optimized correlations for the fix-bed adsorption of metal ions on bone char, *Chem. Eng. Sci.* 55 (2000) 5819–5829.
- [37] V.C. Taty-Costodes, H. Fauduet, C. Porte, Y.S. Ho, Removal of lead(II) ions from synthetic and real effluents using immobilized *Pinus sylvestris* sawdust: Adsorption on a fixed-bed column, *J. Hazard. Mater.* 123 (2005) 135–144.
- [38] T.V.N. Padmesh, K. Vijayaraghavan, G. Sekaran, M. Velan, Batch and column studies on biosorption of acid dyes on fresh water macro alga *Azolla filiculoides*, *J. Hazard. Mater.* 125 (2005) 121–129.